NMRlipids IV: Headgroup & glycerol backbone structures, and cation binding in bilayers with PS lipids

O. H. Samuli Ollila[1,2,*] and NMRlipids collaboration **1.Authorship query to be sent soon.**[3]

[1]*Institute of Organic Chemistry and Biochemistry, Academy of Sciences of the Czech Republic, Prague 6, Czech Republic*
[2]*Institute of Biotechnology, University of Helsinki*
[3]*nmrlipids.blogspot.fi*
(Dated: June 25, 2018)

Primarily measured but also simulated NMR order parameters will be collected also for other than phophatidylcholine (these are discussed in NMRlipids I) headgroup. The information will be used to understand structural differences between different lipid molecules in bilayers.

INTRODUCTION

Phosphatidylserine (PS) is the most common negatively charged lipid in eykaryotic membranes. PS lipids compose 8.5% of total lipid weight of erythrocytes, but the abundance varies between different organelles up to 25-35% in plasma membrane [1–3]. Despite of the relatively low abundance, PS lipids are important signaling molecules. They interact with signaling proteins [2], regulate surface charge and protein localization [4], and induce protein aggregation [5, 6]. Some domains spesifically interact PS lipids, while others are attracted by general electrostatics and the binding can be regulated by calcium [2]. Therefore, the structural details of lipid headgroups and the details of cation binding are crucial for the PS mediated signaling processes.

Previous experimental studies have concluded that PS headgroups have more rigid conformation than phophocholines (PC) due to hydrogen bonding or electrostatic interactions [7, 8]. Multivalent cations and Li^+ are able to form strong dehydrated molecular complexes with PS lipids, while monovalent ions interact more weakly with PS containing bilayers [9–16]. Dilution of bilayers with PC lipids makes PS headgroups less rigid and reduces propensity for the formation of strong complexes with multivalent ions [7, 8, 15, 16].

The structure of PS lipid headgroups and their interactions with ions have been studied with various experimental methods and theoretical techniques [15, 17**?**]. However, the consesus has not been reached due to the difficulties to interpret the experimental data [**?**] and the inaccuracies in simulation models at the headgroup region [18–20]. Some studies propose that the negatively charged lipids attract cations only due to the increase of local concentration in the vicinity of membranes and that the binding constant of cations is similar to zwitterionic and negatively charged lipids [21**?** , 22]. On the other hand, some studies propose specific binding of calcium directly to PS lipid headgroups [23**?** , 24], The NMR data proposes that the PS headgroup is more rigid than PC,PE or PG headgroups, but more detailed interperetation has not been done.

Headgroup and glycerol backbone C-H bond order parameters calculated from MD simulations have been recently used to interpret the lipid structures in NMR experiments and to validate lipid structure and ion binding in simulations of PC lipid bilayers [18–20, 25]. In this work we apply this approach to PS lipid headgroup in order to elucidate the structural details and ion binding to negatively charged lipids. The results are expected to elucidate also PS mediated signalling events because glycerol backbone and headgroup structure and behaviour are similar in model membranes and in bacteria [21, 26, 27].

METHODS

Solid state NMR experiments

The magnitude and signs of the C-H bond order parameters in headgroup and glycerol backbone were measured using natural abundance ^{13}C solid state NMR spectroscopy as described previously [25, 28]. Shortly, the absolute values of the order parameters were determined from the dipolar splittings given by the indirect dimension of 2D R-PDFL experiment [29] and the signs were measured using S-DROSS experiments [30].

2.Details of the used spectrometer and maybe some other details should be given.

3.Sample preparation should be described.

4.How is the peak assignment done?

Molecular dynamics simulations

Molecular dynamics simulation data was collected using the Open Collaboration method [18]. The NMRlipids project blog (`nmrlipids.blogspot.fi`) and the GitHub repository (`github.com/NMRLipids/NMRlipidsIVotherHGs`) were used as the communication platforms. The simulated systems are listed in Table II and simulation details are given in the SI. The simulation data is also indexed in the searchable database (`nmrlipids.fi`), and in the NMRlipids/MATCH GitHub repository (`https://github.com/NMRLipids/MATCH`).

The C-H bond order parameters were calculated directly from the definition

$$S_{CH} = \frac{1}{2}\langle 3\cos^2\theta - 1\rangle, \tag{1}$$

TABLE I: List of MD simulations without additional salt. CKPM refers to the version with Berger/Chiu NH_3 charges compatible with Berger (i.e. the NH_3 group having the same charges as in the $N(CH_3)_3$ group of the PC lipids; 'M' stands for Mukhopadhyay after the first published Berger-based PS simulation that used these charges) and CKP refers to the version with more Gromos compatible version (i.e. the charges for the NH_3 group taken from the lysine side-chain).

lipid/counter-ions	force field for lipids / ions	NaCl (mM)	CaCl$_2$ (mM)	^{a}N$_l$	^{b}N$_w$ **5.**	^{c}N$_c$	^{d}T (K)	^{e}t$_{sim}$(ns)	^{f}t$_{anal}$ (ns)	^{g}files
DOPS/Na$^+$	CHARMM36 [31]	0	0	128	4480	0	303	500	100	[32]
DOPS/Na$^+$	CHARMM36ua [?] **6.**	0	0	128	4480	0	303	500	100	[33]
DOPS/Na$^+$	Slipids [34]	0	0	128	4480	0	303	500	100	[35]
DOPS/Na$^+$	Slipids [34]	0	0	288	11232	0	303	200	100	[36]
DOPS/Na$^+$	Berger [37]	0	0	128	4480	0	303	500	100	[38]
DOPS/Na$^+$	GROMOS-CKP1 [?] **7.**	0	0	128	4480	0	303	500	100	[39]
DOPS/Na$^+$	GROMOS-CKP2 [?] **8.**	0	0	128	4480	0	303	500	100	[40]
DOPS/Na$^+$	lipid17 [41] / JC [42]	0	0	128	4480	0	303	600	100	[43]
DOPS/Na$^+$	lipid17 [41] / ff99 [44]	0	0	128	4480	0	303	600	100	[45]
POPS/Na$^+$	CHARMM36 [31]	0	0	128	4480	0	298	500	100	[46]
POPS/K$^+$	CHARMM36 [31]	0	0	128	4480	0	298	500	100	[47]
POPS/Na$^+$	CHARMM36ua [?] **9.**	0	0	128	4480	0	298	500	100	[48]
POPS/Na$^+$	Slipids [34]	0	0	128	4480	0	298	500	100	[49]
POPS/Na$^+$	Berger [?]	0	0	128	4480	0	298	500	100	[50]
POPS/Na$^+$	MacRog [51]	0	0	?	??	0	?	?	?	[?] **10.**
OPPS/Na$^+$	MacRog [51]	0	0	128	5120	0	298	200	100	[52]
POPS/Na$^+$	GROMOS-CKPM [?] **11.**	0	0	128	4480	0	298	500	100	[53]
POPS/Na$^+$	GROMOS-CKP [?] **12.**	0	0	128	4480	0	298	500	100	[54]
POPS/Na$^+$	lipid17 [41] / JC [42]	0	0	128	4480	0	298	600	100	[55]
POPS/Na$^+$	lipid17 [41] / ff99 [44]	0	0	128	4480	0	298	600	100	[56]

^{a}Number of lipid molecules with largest mole fraction
^{b}Number of water molecules
^{c}Number of additional cations
^{d}Simulation temperature
^{e}Total simulation time
^{f}Time used for analysis
^{g}Reference for simulation files

where θ is the angle between the C-H bond and the membrane normal. Angular brackets point to the average over all sampled configurations. **29.Error estimation should be discussed.**
The number density profiles were calculated using *gmx density* tool from Gromacs sofware package [63].

Comparison of ion binding to negatively charged lipid bilayers between simulations and experiments using the electrometer concept

The order parameters of α and β carbons in PC lipids can be used to measure the ion binding affinity because they decrease proportionally to the amount of bound positive charge to a bilayer [64–66]. This molecular electrometer concept is especially useful for the comparison between simulations and experiments because the headgroup order parameters can be directly calculated from simulations [19]. Also the headgroup order parameters of negatively charged PS and PG lipids exhibit systemic, but less characterized dependence on the bound charge [15, 67–69]. Therefore, the ion binding affinity to negatively charged bilayers can be better characterized measuring the PC headgroup order parameters from mixed bilayers, see section S2 in the supplementary information.

Before using the PC headgroup order parameters to quantify the ion binding affinity, it is important to quantify the response of the headgroup order parameters to the known amount of bound charge [19, 70]. This can be done using the experimental data from the mixtures of monovalent cationic surfactants (dihexadecyldimethylammonium) and POPC [70, 71], see section S3 in the supplementary information. In this work, we also quantify the response of PC headgroup order parameters to the negatively charged PS headgroups, which also follows the electrometer concept in the experiments [27], see section S2 in the supplementary information.

TABLE II: List of MD simulations. The salt concentrations calculated as [salt]=$N_c \times$[water]$/N_w$, where [water] = 55.5 M. CKPM refers to the version with Berger/Chiu NH_3 charges compatible with Berger (i.e. the NH_3 group having the same charges as in the $N(CH_3)_3$ group of the PC lipids; 'M' stands for Mukhopadhyay after the first published Berger-based PS simulation that used these charges [?]) and CKP refers to the version with more Gromos compatible version (i.e. the charges for the NH_3 group taken from the lysine side-chain).

lipid/counter-ions	force field for lipids / ions	NaCl (mM)	CaCl$_2$ (mM)	[a]N_l	[b]N_w 13.	[c]N_c	[d]T (K)	[e]t_{sim}(ns) [f]
POPC:POPS (5:1)/K^+	CHARMM36 [31, 57]	0	0	110:22	4935	0	298	100
POPC:POPS (5:1)/K^+	CHARMM36 [31, 57]	0	0	250:50	?	0	298	200
POPC:POPS (5:1)/K^+	CHARMM36 [31, 57]	0	0	110:22	4620	0	298	500
POPC:POPS (5:1)/Na^+	CHARMM36 [31, 57]	0	0	110:22	4620	0	298	500
POPC:POPS (1:1)/K^+	CHARMM36 [31, 57]	0	0	150:150	?	0	298	200
POPC:POPS (5:1)	CHARMM36 [31, 57, 61]	0	150 17.	250:50	?	?	298	200
POPC:POPS (5:1)	CHARMM36 [31, 57, 61]	0	1000 19.	250:50	?	?	298	200
POPC:POPS21. (5:1)/K^+	MacRog [51]	0	0	120:24	5760	0	298	200
POPC:POPS (5:1)/K^+	MacRog [51]	0	100	120:24	5760	10	298	200
POPC:POPS (5:1)/K^+	MacRog [51]	0	300	120:24	5760	31	298	200
POPC:POPS (5:1)/K^+	MacRog [51]	0	1000	120:24	5760	104	298	200
POPC:POPS (5:1)/K^+	MacRog [51]	0	3000	120:24	5760	311	298	200

27.MacRog simulations with KCl to be added

28.Berger simulations with NaCl and CaCl to be added

[a]Number of lipid molecules with largest mole fraction
[b]Number of water molecules
[c]Number of additional cations
[d]Simulation temperature
[e]Total simulation time
[f]Time used for analysis
[g]Reference for simulation files

RESULTS AND DISCUSSION

Headgroup and glycerol backbone order parameters measured from POPS lipid bilayer

The INEPT and 2D R-PDLF experiments from POPS sample give well resolved spectras for all the carbons in headgroup and glycerol backbone region, except for g_3 for which the resolution was not sufficient to determine the numerical value of the order paramater (Fig. 1). Slices of the R-PDFL spectra (Fig. 1 C)) show a single splitting for the β-carbon with the order parameter value of 0.12, and a superposition of a large and a very small splitting for the α-carbon. The larger splitting gives a order parameter value of 0.09, while the numerical value from the small splitting cannot resolved with the available resolution. Since only the absolute values of the PS headgroup order parameters were measured previously [7, 16], we used the S-DROSS experiment [?] to determine the signs of the order parameters. The S-DROSS slice for the β-carbon (Fig. 1 D)) clearly shows that the order parameter is negative, which is confirmed by SIMPSON simulations. The beginning of the S-DROSS slice suggests that the higher order parameter of the α-carbon is positive and the deviation towards negative values with the longer T_1 times suggests that the smaller order parameter is negative. This is confirmed by a SIMPSON simulation where the value of -0.02 was taken

from ^{2}H NMR experiment [16] for the smaller order parameter. The literature value was used because the resolution of our experiment was not sufficient to determine the small value of the order parameter. The S-DROSS curve from SIMPSON simulation with a positive value for the smaller order parameter (dashed grey in Fig. 1 D)) did not agree with the experiment, confirming the interpretation that the smaller order parameter is negative.

The headgroup and glycerol backbone order parameters of POPS measured in this work are in good agreement with the previously reported values from ^{2}H NMR experiments of DOPS [7] (Fig. 2). The β-carbon order parameter is significantly more negative and α-carbon experiences a significant forking in PS headgroup when compared with the values previously measured for POPC [28] (Fig. 2). These features have been intepreted to arise from a rigid PS headgroup conformation, stabilized by hydrogen bonds or electrostatic interactions [7, 8], but detailed structrural interpretation is not available.

Headgroup and glycerol backbone in simulations of PS lipid bilayers without additional ions

The headgroup order parameters of DOPS and POPS bilayers from different simulation models are compared with the experimental data in Fig. 3. Subjective ranking of the quality of the models is shown in Fig. 4. The tested models perform
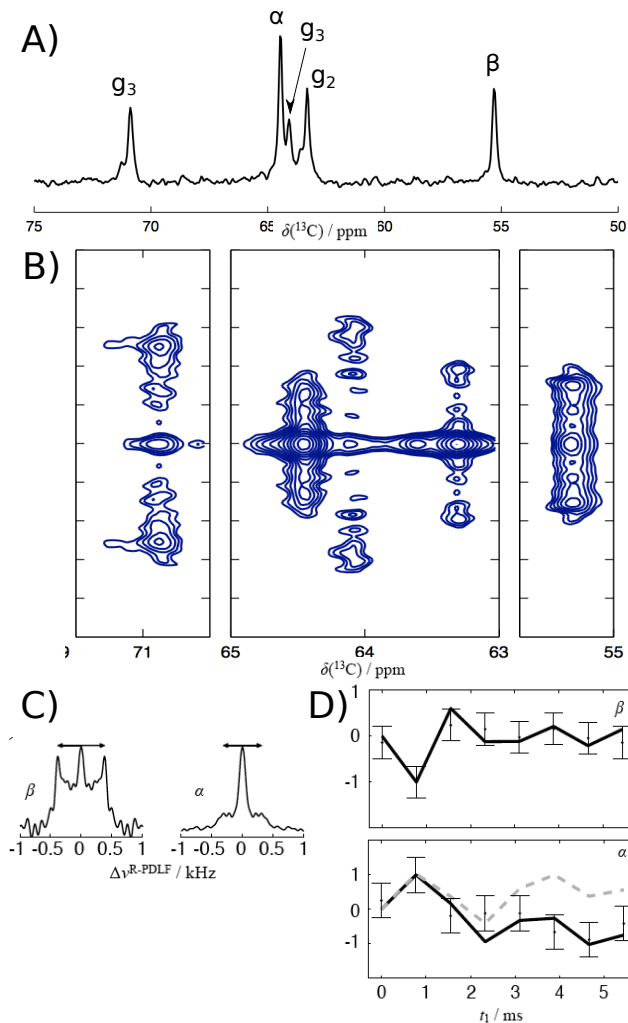
FIG. 1: (a) The headgroup region of the INEPT spectrum with headgroup and glycerol backbone carbons assigned. (b) 2D R-PDLF spectra for headgroup and glycerol backbone regions. (c) Slices for α and β barbons. (d) Experimental SDROSS data (points) and SIMPSON simulations (lines). Order parameter values of -0.12 for the β-carbon, and 0.09 and -0.02 for the larger and smaller α-carbon slittings were used in the SIMPSON calculations. The S-DROSS curve from SIMPSON simulation with positive value for the smaller order parameter (dashed grey).

30.This is preliminary figure, should be polished. 31.Should we show slices for all the analyzed carbons in (c)?

generally less well than in the previous study for PC headgroup [18] and none of the models reproduce the experimental order parameters within experimental error bars. Therefore, the models cannot be straightforwardly used to interpret the structure of PS headgroup. However, the differences between PC and PS headgroups are partially reproduced by some of the models.

The two best performing models for the α and β-carbons of PS, Slipids and CHARMM36, reproduce the large forking in the α-carbon and the Slipids model gives also a good agreement with experiments for the β-carbon order parameter
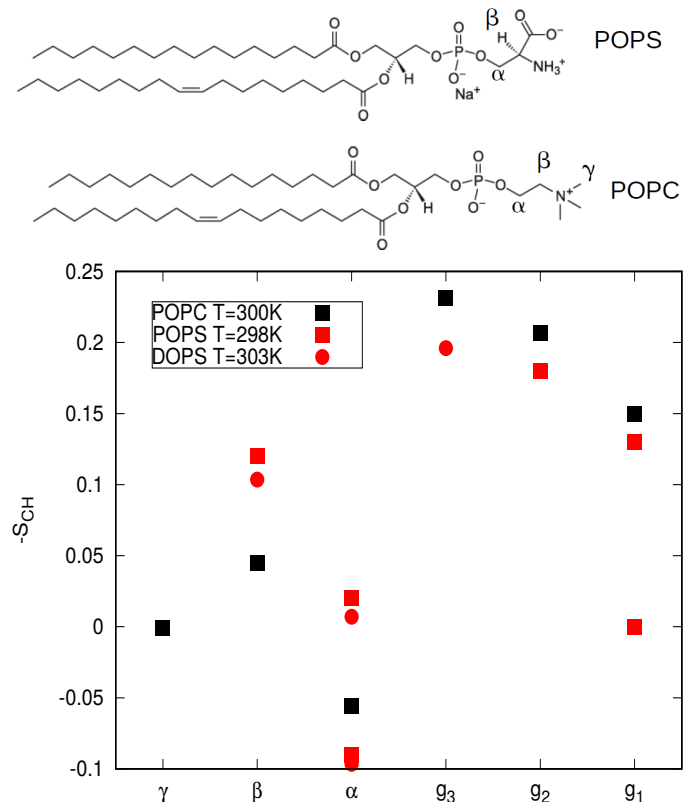
FIG. 2: Headgroup and glycerol backbone order parameters of POPS measured in this work compared with values for DOPS (^{2}H NMR, 0.1M of NaCl) [7] and POPC (^{13}C NMR) [28] from literature. Signs for PS order parameters as measured in this work and signs for PC as measured in Refs [25 **?**].

32.There should be values in [15] which should be added.

in both PC and PS headgroups (Fig. 3 and Ref. 18). Interestingly, the dihedral angle distributions of CHARMM36 and Slipids in Fig. S7 share significant similarities in the headgroup region. However, the experimental order parameters in the glycerol backbone region are not well reproduced by the Slipids model, which was also the case in for PC lipids [18]. This difference probably arises from the differences in the dihedral angle distributions of C1-C2-C3-O31 and C2-C3-O31-C31 in Figure S6, which are also illustrated in Figure 5.

35.Also the discussion about POPS/OPPS issue with MacRog model should be added.

Counterion binding to lipid bilayers containing PS lipids

Membranes containing PS lipids are always accomppanied with counterions, which modulate electrostatic interactions between lipids and other biomolecules. Counterions are also suggested screen the repulsion between charged lipid headgroups in MD simulations and reduce the area per lipid of PS bilayers to be smaller than in PC bilayers [37, 72, 73]. The counterion density profiles along membrane normal show significant differences between simulation models (Fig. 6).
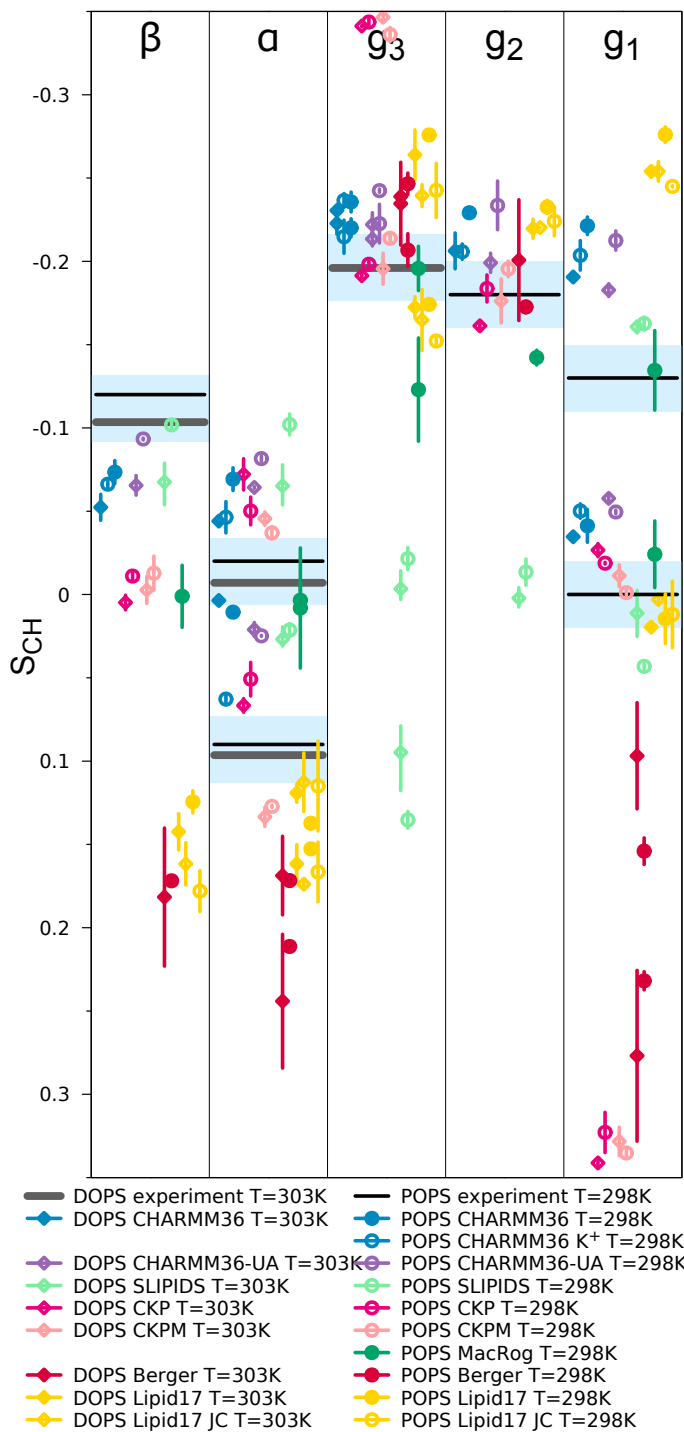
FIG. 3: Order parameters for PS headgroup and glycerol backbone from simulations with different models and experiments without $CaCl_2$. All DOPS data at 303 K, POPS at 298 K. Experimental data from [7] contain 0.1 M of NaCl. Signs are taken from experiments for POPS described in Supplementary Information. The vertical bars shown are not error bars, but demonstrate that we had at least two data sets; the ends of the bars mark the extreme values from the sets, and the dot marks their measurement-time-weighted average.

	β	α	g_3	g_2	g_1	Σ
CHARMM 36	M	M F	M	M	M F	8
CHARMM 36-UA	M	M	M	M	M F	8
GROMOS-CKP1	M	M F	M F		M F	14
GROMOS-CKP2	M	M F	M F		M F	14
Slipid	M	M	M F	M	M F	14
Berger	M	M F	M F	M	M F	15

FIG. 4: Rough subjective ranking of force fields based on Figure 3. Here M indicates a magnitude problem, F a forking problem; letter size increases with problem severity. Color scheme: within experimental error (dark green), almost within experimental error (light green), clear deviation from experiments (light red), and major deviation from experiments (dark red). The Σ-column shows the total deviation of the force field, when individual carbons are given weights of 0 (matches experiment), 1, 2, and 4 (major deviation). For full details of the assessment, see Supplementary Information.

33.Issue about possible updates to this plot:
https://github.com/NMRlipids/NMRlipidsIVotherHGs/issues/4
34.Lipid17 and MacRog results should be added into this plot.
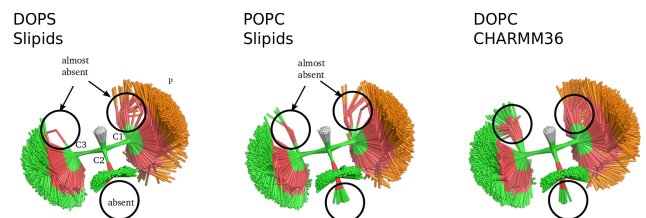
FIG. 5: Snapshots overlayed from different simulations for glycerol backbone region by Pavel Buslaev.

The strongest counterion binding, i.e., the lowest concentrations in bulk water, are observed in MacRog, Berger and Lipid17/JC simulations. CHARMM36, CHARMM36ua and Gromos-CKP models exhibit two local maxima in counterion density, while a single maxima is observed in the other models. **36.More detailed discussion may be possible after comparing monovalent ion binding to bilayers between CHARMM simulations and experiments.** Area per lipid is in agreement with experiments [74] only in the Gromos-CKP models, while other models give significantly lower values (Fig. 6). The difference cannot be explained by the electrostatic screening of the headgroup repulsion due to counterion binding because CHARMM36, CHARMM36ua
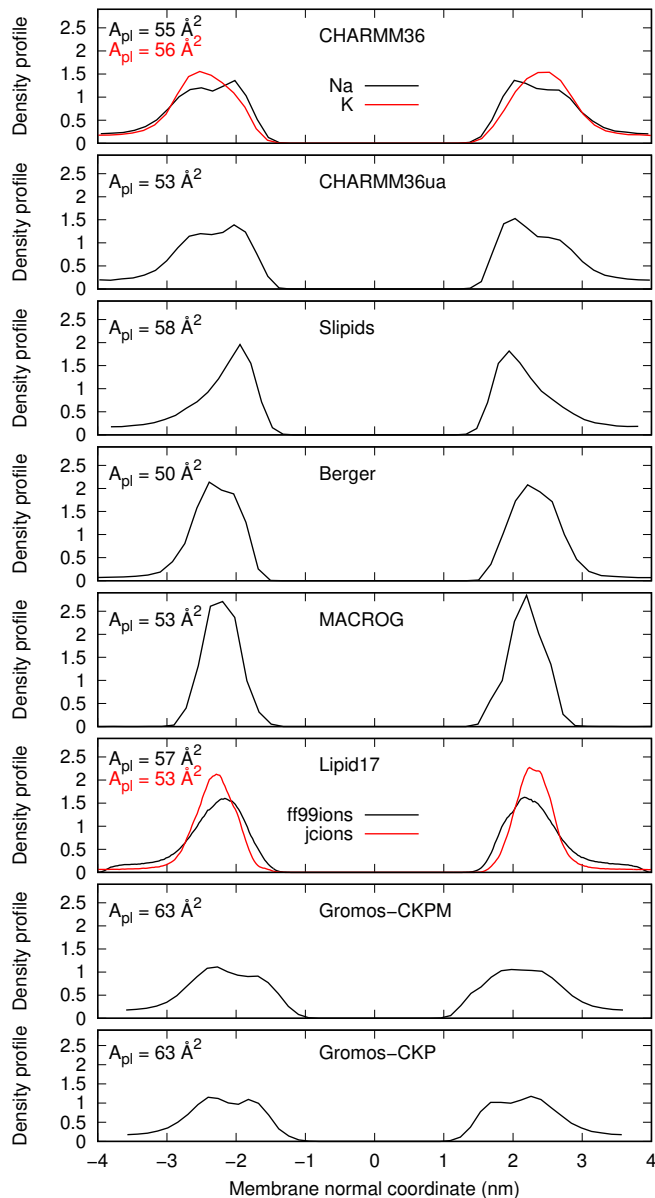
FIG. 6: Counterion densities of POPS lipid bilayer along the membrane normal from simulations with different force fields.

groups [75]. This is evident also in the changes of PS headgroup order parameters, which decrease with the addition of lithium but increase with the addition of sodium or potassium (Fig. 7). POPC headgroup order parameters exhibit a clear decrease as a function of LiCl concentration but only modest changes as a function of KCl concentration, indicating significant Li^+ binding but only weak Na^+ binding to the mixture when interpreted using the electrometer concept [64–66]. In simulations with the Berger model, the headgroup order parameter response of POPC to the added NaCl is similar to the experiments of LiCl, indicating overestimated binding affinity of sodium, in line with the results for PC bilayers [19]. Indeed, the sodium density profile shows a significant binding peak in the Berger model (Fig. 8). Potassium binding in the MacRog simulation is significantly weaker (Fig. 8) and the headgroup order parameter changes are also in better agreement with simulations (Fig. 7). **37.Discussion about Lipid17 to be written when we have the density profiles.** All the tested models overestimate the changes of POPS headgroup order parameters as a function of monovalent ions (Fig. 7), suggesting that model development is necessary to interpret the PS headgroup-ion interactions from MD simulations.

Headgroup structure in PS and PC mixtures

Dilution of PS lipid bilayers with PC lipids reduces the propensity of PS headgroup-multivalent ion complexes and is proposed to make PS headgroups less rigid [7, 8, 15, 16]. Therefore, the intermolecular interactions at the headgroup region seems to be important for the physical properties of mixed lipid bilayers. These interactions can be indirectly monitored by measuring the headgroup order parameters from PS:PC mixtures with different molar ratios. The headgroup order parameters of POPC increase in such experiments with increasing amount of POPS (Fig. 9) [27]. This behaviour is generally observed when negatively charged lipids or surfactants are mixed with PC lipids [27, 71] and can be understood by the tilting of lipid headgroup more parallel to the membrane plane according to the electrometer concept [66]. The headgroup order parameters of PS lipids shift closer to zero when bilayer is diluted with PC lipids in experiments (Fig. 9) [7, 15, 27], which is intepreted to indicate reduced rigidity [7, 8].

The increase of POPC headgroup order parameters with the increasing amount of negatively charged POPS lipid is reproduced in MacRog simulations with potassium counterions, but not in Berger simulations with sodium or in CHARMM36 simulations with potassium or sodium conterions (Fig. 9). The observations can be explained using the electrometer concept. The Berger simulation exhibits very strong sodium binding (Fig. 8), which surpasses the effect of negatively charged lipids as also the amount of counterions increase with increasing amount of PS. In CHARMM36 simulations, the counterion binding neutralizes the effect of PS and the headgroup order parameters are not changed with increasing amount of

and Slipid models give smaller area per lipid than Gromos-CKP models with similar counterion binding affinity.

To evaluate counterion binding in different simulation models against experimental data [15], we plot the headgroup order parameters measured from POPC:POPS 5:1 mixture as a function of different monovalent ions added to the buffer (Fig. 7). Experimental order parameter data for POPC headgroup in the mixture is available as a function of LiCl and KCl concentrations, while POPS headgroup order parameters are measured also as a function of NaCl. Lithium interacts more strongly with PS headgroups than other monovalent ions [11, 12, 14, 15, 69], as also observed for PC head-
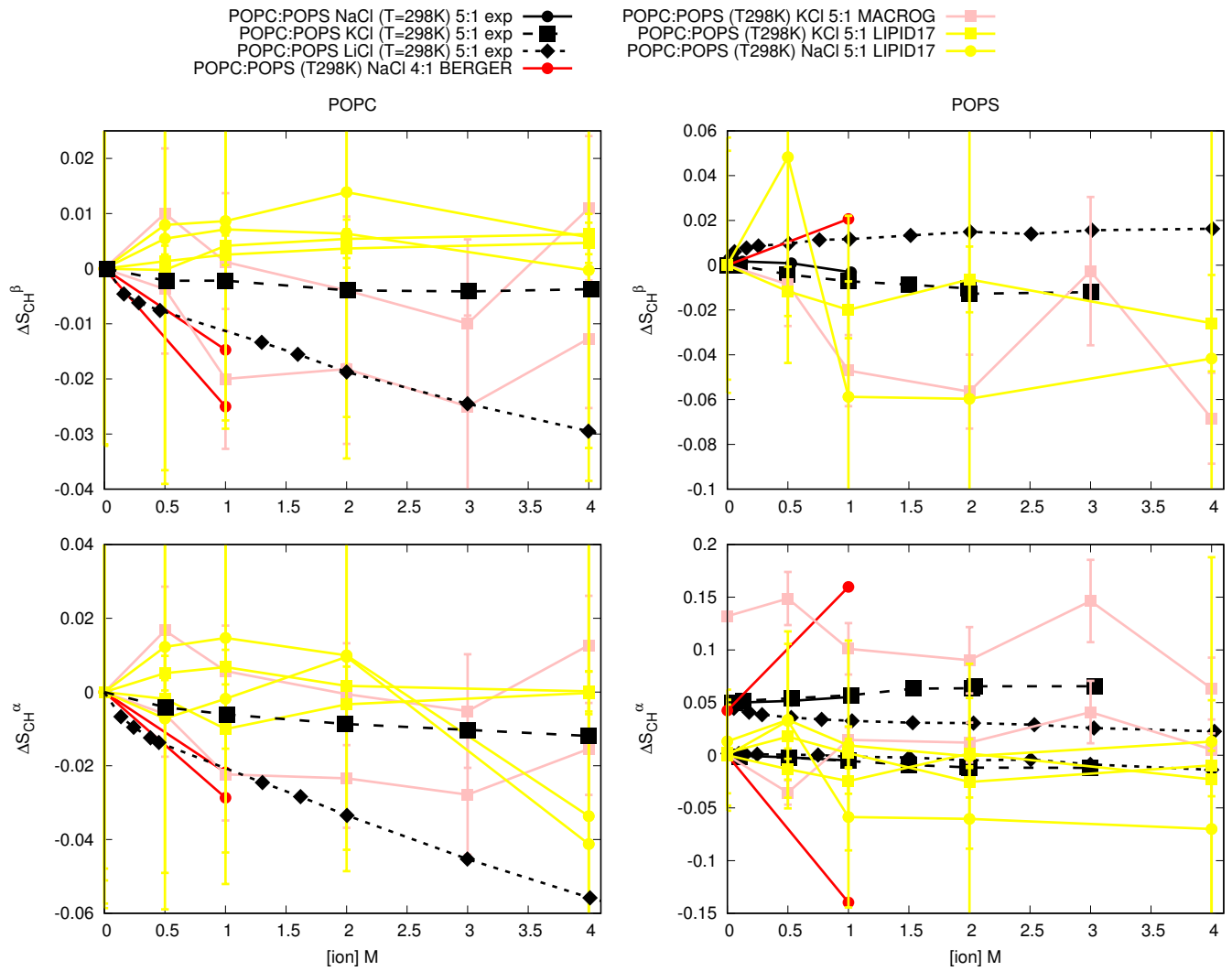
FIG. 7: Changes of the PC (left) and PS (right) headgroup order parameters as a function of added NaCl, KCl and LiCl from POPC:POPS (5:1) mixture. The experimental data is from Ref. 15. The values from counterion-only systems are set as a zero point of y-axis. To correctly illustrate the significant forking of the α-carbon order parameter in PS headgroup (bottom, right), the y-axis is tranferred with the same value for both order parameters such that the lower order parameter value is at zero.

38.CHARMM36 results for this plot would be highly useful.

PS. Finally, the weak binding of potassium in the MacRog simulations enables the increase of order parameters with the increasing amount of negatively charged PS lipids (Figs. 9 and 8).

Oppositely to experiments, the headgroup order parameter of POPS shift away from zero in CHARM36 simulations when bilayer is diluted with POPC (Fig. 9). In lipid14/17 simulations, the POPS order parameter shift closer to zero when bilayer is diluted with POPC, but the numerical values of order parameters are too far from experiments to enable interpretation of the experimental data. Therefore, we conlcude that the force field development is necessary before MD simulations can be used to interpret the interactions between PC and PS headgroups.

Ca^{2+} binding affinity in bilayers with negatively charged PS lipids

The dehydrated complexes of PS headgroup and calcium ions can also lead to the phase separation [9, 10, 12–16]. Therefore, the Ca2+ binding affinity to PS lipids containing bilayers is easier to study using mixtures diluted with PC lipids [15, 16], where the lipid-ion complexes and phase separation are not observed [13–16]. The decrease of POPC headgroup order parameters as a function of Ca^{2+} concentration in the POPC:POPS (5:1) mixture is overestimated in all the tested simulation models when compared with experiments [15], except in the CHARMM36 simulations with special NBfix [61] for calcium which underestimate the change (Fig. 10). According to the electrometer con-
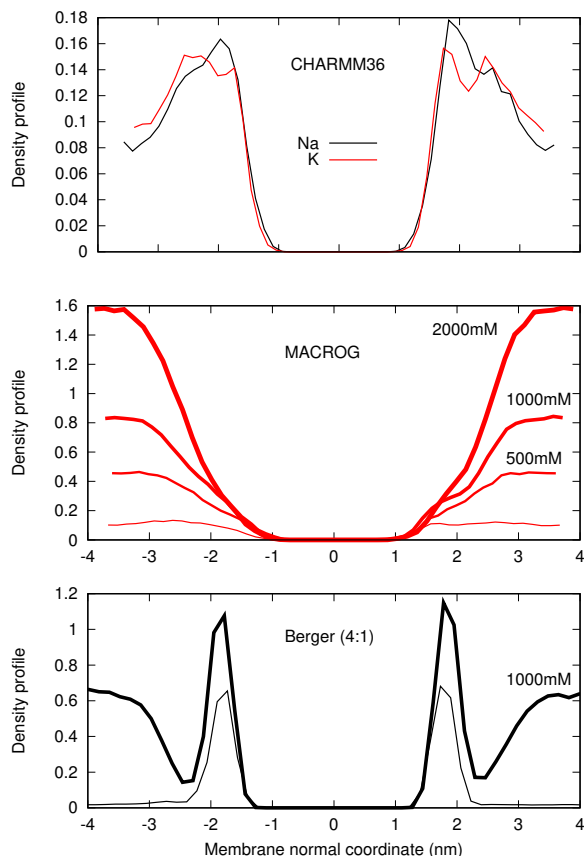
FIG. 8: Counterion density distributions from PC:PS mixtures.

39.Lipid 17 is to be added.

parameter of POPS decrease and the smaller one slightly increase with the added $CaCl_2$ in the experiment. The changes are again significantly overestimated in the simulations, however, in this case all simulations predict qualitatively different behaviour. Notably, the changes of POPS headgroup order parameters are overestimated also in the CHARMM36/NBfix model where the calcium binding affinity was too low. We conclude that the effect of bound ions to the headgroup order parameters of POPS is not qualitatively reproduced by the tested simulations models. This is in contrast to previous results for PC headgroup [19], where qualitatively correct reponse to bound ions was observed despite of significant discrepancies in the headgroup structure without additional ions. The response of POPS headgroup order parameters to the bound charge is systematic but less well understood than the responce of PC headgroups used in the electrometer concept [15, 66]. The force field development is necessary to generate MD simulations that could be used to explain the interactions between PS headgroup and calcium ions.

CONCLUSIONS

cept, this means that the calcium binding seen in the ion density distributions along membrane normal (Fig. 11) is underestimated in the CHARMM36/NBfix model, but overestimated in the other tested models. The overbinding of Ca^{2+} in simulations is expected based on previous study of PC lipid bilayers [19], but underestimated calcium binding affinity in CHARMM36/NBfix model is surprising because CHARMM36 predicted overestimated binding to PC bilayers. The difference can be explained by the NBfix interaction parameters from Ref. 61, incorporated in the parameters give by the CHARMM-GUI at the time of running the simulations (January 2018). These parameters underestimate also the binding of calcium to pure POPC bilayers (Figs. S9 and S10).

The headgroup order parameters of POPS headgroup measured from POPC:POPS (5:1) mixture exhibit a strong dependence of $CaCl_2$ with small concentrations with a rapid saturation below 100 mM (Fig. 10). The β-carbon order parameter of POPS increase with the added $CaCl_2$ in the experiment and in all the tested simulation models, but simulations significantly overestimated the change. The larger α-carbon order
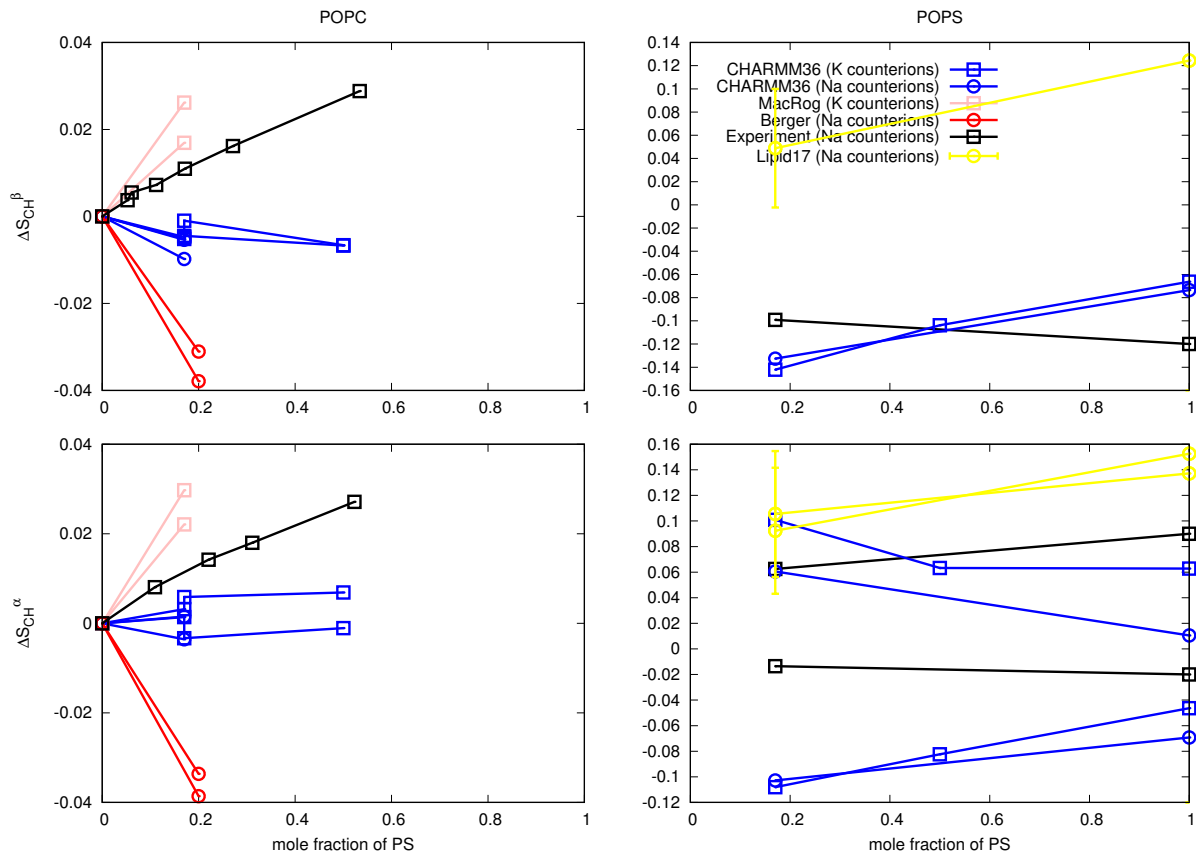
FIG. 9: Changes of PC (left panel) and PS (right panel) headgroup order parameters from POPC:POPS mixtures with increasing amount of POPS. Experimental results of POPC are taken from Ref. 27 (signs are determined as discussed in [18, 20]). Experimental values for POPS in pure bilayer and in mixture are measured in this work and in Ref. 15 at 298K, respectively. Since the experimental data of POPS in pure and diluted mixture come from different experimental sets (13C NMR in this work and 2H NMR from Ref. 15), the experimental change of the order parameter is less accurate than in typical measurements where same technique is used in all conditions, see discussion about qualitative and quantitative accuracy in Ref. 20. For POPC (left panel) the zero point of y-axis is set to the value of pure bilayer. For β-carbon of POPS (right panel, top) the zero point of y-axis is set to the value from POPC:POPS (5:1) mixture. For α-carbon of POPS (right panel, bottom) the y-axis is tranferred with the same value for both order parameters such that the lower order parameter value from POPC:POPS (5:1) mixture is at zero to correctly illustrate the significant forking.

40.Simulation of CHARMM36 at 298K should be maybe rerun with Gromacs 5.

41.Simulation of pure POPC at 298K with Lipid14 would be useful for this plot (only at 303 K is available from NMRlipids I)

42.MacRog simulations of pure POPS with potassium counterions only would be useful for this and other plots.

* samuli.ollila@helsinki.fi
[1] M. A. Lemmon, Nat. Rev. Mol. Cell Biol. **9**, 99 (2008).
[2] P. A. Leventis and S. Grinstein, Annual Review of Biophysics **39**, 407 (2010).
[3] L. Li, X. Shi, X. Guo, H. Li, and C. Xu, Trends in Biochemical Sciences **39**, 130 (2014), ISSN 0968-0004.
[4] T. Yeung, G. E. Gilbert, J. Shi, J. Silvius, A. Kapus, and S. Grinstein, Science **319**, 210 (2008).
[5] H. Zhao, E. K. J. Tuominen, and P. K. J. Kinnunen, Biochemistry **43**, 10302 (2004).
[6] G. P. Gorbenko and P. K. Kinnunen, Chemistry and Physics of Lipids **141**, 72 (2006).
[7] J. L. Browning and J. Seelig, Biochemistry **19**, 1262 (1980).
[8] G. Büldt and R. Wohlgemuth, The Journal of Membrane Biol-

ogy **58**, 81 (1981), ISSN 1432-1424, URL http://dx.doi.org/10.1007/BF01870972.
[9] H. Hauser, E. Finer, and A. Darke, Biochemical and Biophysical Research Communications **76**, 267 (1977), ISSN 0006-291X, URL http://www.sciencedirect.com/science/article/pii/0006291X77907215.
[10] R. J. Kurland, Biochemical and Biophysical Research Communications **88**, 927 (1979), ISSN 0006-291X, URL http://www.sciencedirect.com/science/article/pii/0006291X79914979.
[11] H. Hauser and G. G. Shipley, Biochemistry **22**, 2171 (1983).
[12] H. Hauser and G. Shipley, Biochimica et Biophysica Acta (BBA) - Biomembranes **813**, 343 (1985), ISSN 0005-2736, URL http://www.sciencedirect.com/science/article/pii/0005273685902512.
[13] G. W. Feigenson, Biochemistry **25**, 5819 (1986).
[14] J. Mattai, H. Hauser, R. A. Demel, and G. G. Shipley, Biochem-
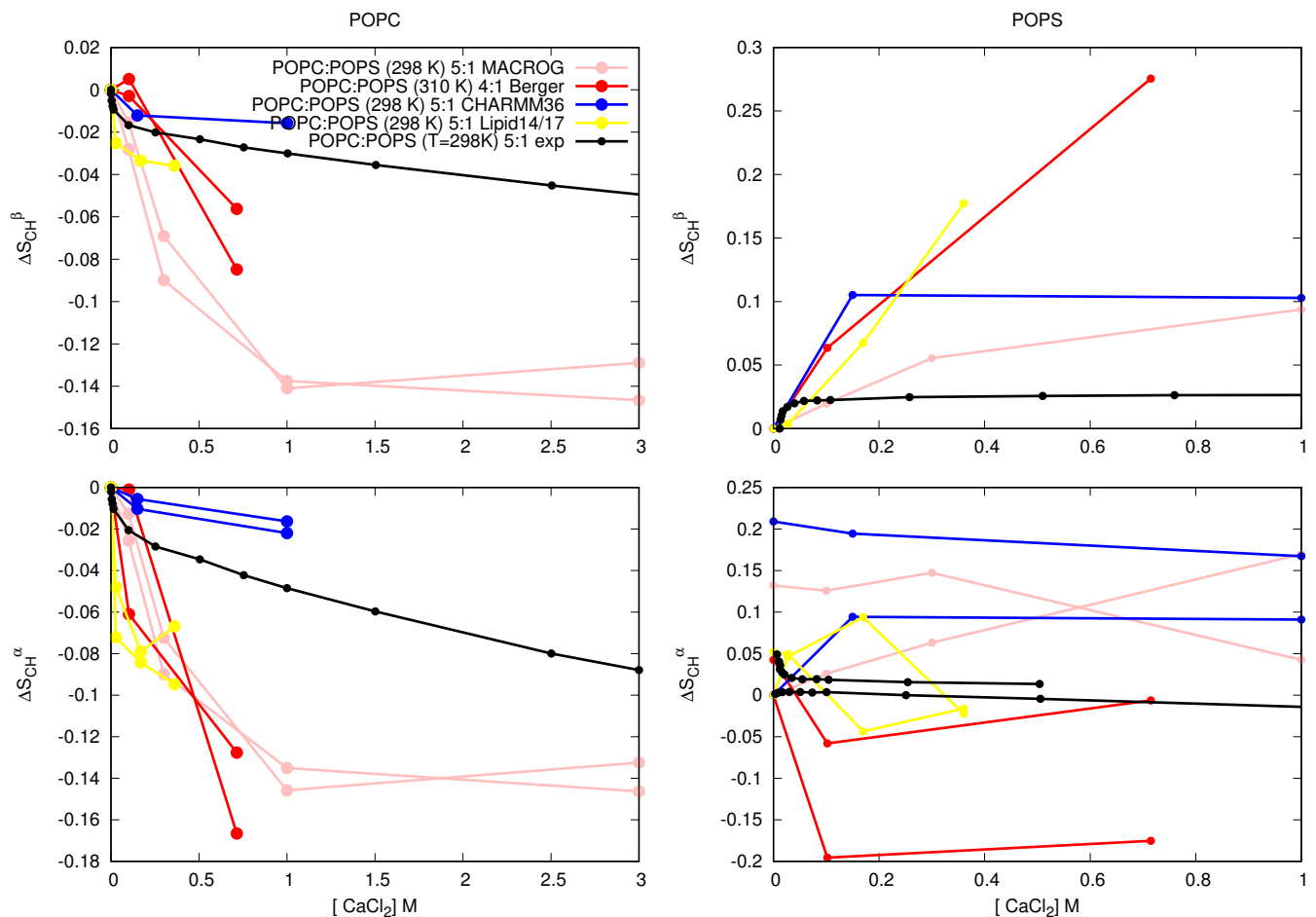
FIG. 10: Changes of POPC (left) and POPS (right) headgroup order parameters in POPC:POPS (5:1) mixture as a function CaCl$_2$ concentration. Experimental data is taken from 15. The values from counterion-only systems are set as a zero point of y-axis. To correctly illustrate the significant forking of the α-carbon order parameter in PS headgroup (bottom, right), the y-axis is tranferred with the same value for both order parameters such that the lower order parameter value is at zero.

43.Information about the cuonterions in different simulations should be added

44.Upcoming simulations with original CHARMM36 have been mentioned in the blog:

http://nmrlipids.blogspot.com/2017/12/nmrlipids-iv-current-status-and.html?showComment=1520090718976#c5569269391707740056

45.Upcoming Lipid17 simulations have been mentioned in the blog

http://nmrlipids.blogspot.com/2017/12/nmrlipids-iv-current-status-and.html?showComment=1515177306419#c994825612316235467

istry **28**, 2322 (1989).

[15] M. Roux and M. Bloom, Biochemistry **29**, 7077 (1990).

[16] M. Roux and M. Bloom, Biophys. J. **60**, 38 (1991).

[17] A. Melcrová, S. Pokorna, S. Pullanchery, M. Kohagen, P. Jurkiewicz, M. Hof, P. Jungwirth, P. S. Cremer, and L. Cwiklik, Sci. Reports **6**, 38035 (2016).

[18] A. Botan, F. Favela-Rosales, P. F. J. Fuchs, M. Javanainen, M. Kanduč, W. Kulig, A. Lamberg, C. Loison, A. Lyubartsev, M. S. Miettinen, et al., J. Phys. Chem. B **119**, 15075 (2015).

[19] A. Catte, M. Girych, M. Javanainen, C. Loison, J. Melcr, M. S. Miettinen, L. Monticelli, J. Maatta, V. S. Oganesyan, O. H. S. Ollila, et al., Phys. Chem. Chem. Phys. **18**, 32560 (2016).

[20] O. S. Ollila and G. Pabst, Biochimica et Biophysica Acta (BBA) - Biomembranes **1858**, 2512 (2016).

[21] J. Seelig, Cell Biology International Reports **14**, 353 (1990), ISSN 0309-1651, URL http://www.sciencedirect. com/science/article/pii/030916519091204H.

[22] C. G. Sinn, M. Antonietti, and R. Dimova, Colloids and Surfaces A: Physicochemical and Engineering Aspects **282-283**, 410 (2006), a Collection of Papers in Honor of Professor Ivan B. Ivanov (Laboratory of Chemical Physics and Engineering, University of Sofia) Celebrating his Contributions to Colloid and Surface Science on the Occasion of his 70th Birthday.

[23] P. T. Vernier, M. J. Ziegler, and R. Dimova, Langmuir **25**, 1020 (2009).

[24] J. M. Boettcher, R. L. Davis-Harrison, M. C. Clay, A. J. Nieuwkoop, Y. Z. Ohkubo, E. Tajkhorshid, J. H. Morrissey, and C. M. Rienstra, Biochemistry **50**, 2264 (2011).

[25] T. M. Ferreira, R. Sood, R. Bärenwald, G. Carlström, D. Topgaard, K. Saalwächter, P. K. J. Kinnunen, and O. H. S. Ollila, Langmuir **32**, 6524 (2016).

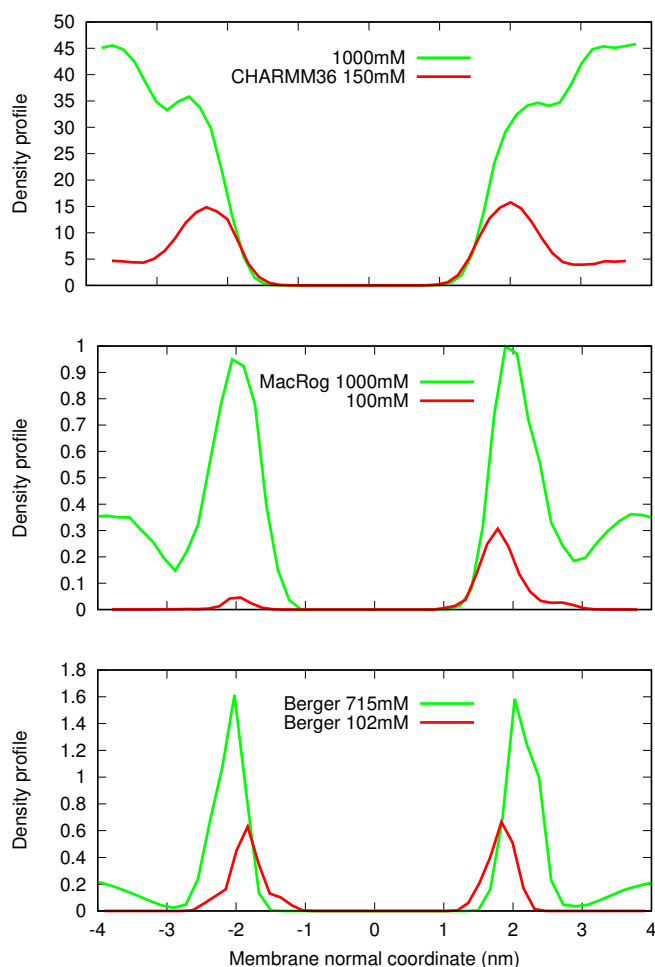[26] H. U. Gally, G. Pluschke, P. Overath, and J. Seelig, Biochem-

FIG. 11: Ca2+ density profiles from simulations.

46.The CHARMM results are mass densities, numbers should be used.

47.Should we include also counterions into the plot?

48.Not all the data from MacRog is included.

istry **20**, 1826 (1981).

[27] P. Scherer and J. Seelig, EMBO J. **6** (1987).

[28] T. M. Ferreira, F. Coreta-Gomes, O. H. S. Ollila, M. J. Moreno, W. L. C. Vaz, and D. Topgaard, Phys. Chem. Chem. Phys. **15**, 1976 (2013).

[29] S. V. Dvinskikh, H. Zimmermann, A. Maliniak, and D. Sandstrom, J. Magn. Reson. **168**, 194 (2004).

[30] J. D. Gross, D. E. Warschawski, and R. G. Griffin, J. Am. Chem. Soc. **119**, 796 (1997).

[31] R. M. Venable, Y. Luo, K. Gawrisch, B. Roux, and R. W. Pastor, The Journal of Physical Chemistry B **117**, 10183 (2013).

[32] T. Piggot, *CHARMM36 DOPS simulations (versions 1 and 2) 303 K 1.0 nm LJ switching* (2017), URL https://doi.org/10.5281/zenodo.1129411.

[33] T. Piggot, *CHARMM36-UA DOPS simulations (versions 1 and 2) 303 K 1.0 nm LJ switching* (2017), URL https://doi.org/10.5281/zenodo.1129456.

[34] J. P. M. Jämbeck and A. P. Lyubartsev, Phys. Chem. Chem.

Phys. **15**, 4677 (2013).

[35] T. Piggot, *Slipids DOPS simulations (versions 1 and 2) 303 K 1.0 nm cut-off with LJ-PME* (2017), URL https://doi.org/10.5281/zenodo.1129439.

[36] F. Favela-Rosales, *MD simulation trajectory of a fully hydrated DOPS bilayer: SLIPIDS, Gromacs 5.0.4. 2017.* (2017), URL https://doi.org/10.5281/zenodo.495510.

[37] P. Mukhopadhyay, L. Monticelli, and D. P. Tieleman, Biophysical Journal **86**, 1601 (2004).

[38] T. Piggot, *Berger DOPS simulations (versions 1 and 2) 303 K 1.0 nm cut-off* (2017), URL https://doi.org/10.5281/zenodo.1129419.

[39] T. Piggot, *GROMOS-CKP DOPS simulations (versions 1 and 2) 303 K with Berger/Chiu NH3 charges and PME* (2017), URL https://doi.org/10.5281/zenodo.1129429.

[40] T. Piggot, *GROMOS-CKP DOPS simulations (versions 1 and 2) 303 K with GROMOS NH3 charges and PME* (2017), URL https://doi.org/10.5281/zenodo.1129447.

[41] I. Gould, A. Skjevik, C. Dickson, B. Madej, and R. Walker, *Lipid17: A comprehensive amber force field for the simulation of zwitterionic and anionic lipids* (2018), in preparation.

[42] I. S. Joung and T. E. Cheatham, The Journal of Physical Chemistry B **112**, 9020 (2008).

[43] B. Kav and M. S. Miettinen, *Molecular dynamics simulation trajectory of an anionic lipid bilayer: 100 mol% DOPS with Na+ counterions using Joung-Cheetham Ions* (2018), B.K acknowledges financial support from International Max Planck Research School on Multiscale Bio-Systems, URL https://doi.org/10.5281/zenodo.1134871.

[44] J. Åqvist, J. Phys. Chem. **94**, 8021 (1990).

[45] B. Kav and M. S. Miettinen, *Molecular dynamics simulation trajectory of an anionic lipid bilayer: 100 mol% DOPS with Na+ counterions using ff99 Ions* (2018), B.K acknowledges financial support from International Max Planck Research School on Multiscale Bio-Systems, URL https://doi.org/10.5281/zenodo.1135142.

[46] T. Piggot, *CHARMM36 POPS simulations (versions 1 and 2) 298 K 1.0 nm LJ switching* (2017), URL https://doi.org/10.5281/zenodo.1129415.

[47] T. Piggot, *CHARMM36 POPS simulations (versions 1 and 2) 298 K 1.0 nm LJ switching with K ions* (2018), URL https://doi.org/10.5281/zenodo.1182654.

[48] T. Piggot, *CHARMM36-UA POPS simulations (versions 1 and 2) 298 K 1.0 nm LJ switching* (2017), URL https://doi.org/10.5281/zenodo.1129458.

[49] T. Piggot, *Slipids POPS simulations (versions 1 and 2) 298 K 1.0 nm cut-off with LJ-PME* (2017), URL https://doi.org/10.5281/zenodo.1129441.

[50] T. Piggot, *Berger POPS simulations (versions 1 and 2) 298 K 1.0 nm cut-off* (2017), URL https://doi.org/10.5281/zenodo.1129425.

[51] A. Maciejewski, M. Pasenkiewicz-Gierula, O. Cramariuc, I. Vattulainen, and T. Róg, J. Phys. Chem. B **118**, 4571 (2014).

[52] M. Javanainen, *Simulation of a pops bilayer* (2017), URL https://doi.org/10.5281/zenodo.1120287.

[53] T. Piggot, *GROMOS-CKP POPS simulations (versions 1 and 2) 298 K with Berger/Chiu NH3 charges and PME* (2017), URL https://doi.org/10.5281/zenodo.1129431.

[54] T. Piggot, *GROMOS-CKP POPS simulations (versions 1 and 2) 298 K with GROMOS NH3 charges and PME* (2017), URL https://doi.org/10.5281/zenodo.1129435.

[55] M. S. Miettinen and B. Kav, *Molecular dynamics simulation trajectory of an anionic lipid bilayer: 100 mol% POPS with Na+ counterions using Joung-Cheatham Ions* (2018), B.K. ac-

knowledges financial support from International Max Planck Research School on Multiscale Bio-Systems., URL `https://doi.org/10.5281/zenodo.1148495`.

[56] M. S. Miettinen and B. Kav, *Molecular dynamics simulation trajectory of an anionic lipid bilayer: 100 mol% POPS with Na+ counterions using ff99 ions* (2018), B.K. acknowledges financial support from International Max Planck Research School on Multiscale Bio-Systems, URL `https://doi.org/10.5281/zenodo.1134869`.

[57] J. B. Klauda, R. M. Venable, J. A. Freites, J. W. O'Connor, D. J. Tobias, C. Mondragon-Ramirez, I. Vorobyov, A. D. MacKerell Jr, and R. W. Pastor, J. Phys. Chem. B **114**, 7830 (2010).

[58] O. H. S. Ollila, *POPS+83%popc lipid bilayer simulation at T298K ran CHARMM_GUI force field and Gromacs* (2017), URL `https://doi.org/10.5281/zenodo.1011104`.

[59] T. Piggot, *CHARMM36 POPS/POPC simulations (versions 1 and 2) 298 K 1.0 nm LJ switching with K ions* (2018), URL `https://doi.org/10.5281/zenodo.1182658`.

[60] T. Piggot, *CHARMM36 POPS/POPC simulations (versions 1 and 2) 298 K 1.0 nm LJ switching with Na ions* (2018), URL `https://doi.org/10.5281/zenodo.1182665`.

[61] S. Kim, D. Patel, S. Park, J. Slusky, J. Klauda, G. Widmalm, and W. Im, Biophysical Journal **111**, 1750 (2016), ISSN 0006-3495, URL `http://www.sciencedirect.com/science/article/pii/S0006349516307615`.

[62] M. Javanainen, *Simulations of popc/pops membranes with cacl_2.* (2017), URL `https://doi.org/10.5281/zenodo.897467`.

[63] M. Abraham, D. van der Spoel, E. Lindahl, B. Hess, and the GROMACS development team, *GROMACS user manual version 5.0.7* (2015), URL `www.gromacs.org`.

[64] H. Akutsu and J. Seelig, Biochemistry **20**, 7366 (1981).

[65] C. Altenbach and J. Seelig, Biochemistry **23**, 3913 (1984).

[66] J. Seelig, P. M. MacDonald, and P. G. Scherer, Biochemistry **26**, 7535 (1987).

[67] F. Borle and J. Seelig, Chemistry and Physics of Lipids **36**, 263 (1985).

[68] P. M. Macdonald and J. Seelig, Biochemistry **26**, 1231 (1987).

[69] M. Roux and J.-M. Neumann, FEBS Letters **199**, 33 (1986).

[70] J. Melcr, H. Martinez-Seara, R. Nencini, J. Kolafa, P. Jungwirth, and O. H. S. Ollila, The Journal of Physical Chemistry B **122**, 4546 (2018).

[71] P. G. Scherer and J. Seelig, Biochemistry **28**, 7720 (1989).

[72] S. A. Pandit and M. L. Berkowitz, Biophysical Journal **82**, 1818 (2002).

[73] U. R. Pedersen, C. Leidy, P. Westh, and G. H. Peters, Biochimica et Biophysica Acta (BBA) - Biomembranes **1758**, 573 (2006).

[74] J. Pan, X. Cheng, L. Monticelli, F. A. Heberle, N. Kucerka, D. P. Tieleman, and J. Katsaras, Soft Matter **10**, 3716 (2014).

[75] G. Cevc, Biochim. Biophys. Acta - Rev. Biomemb. **1031**, 311 (1990).

ToDo